J Mater Sci: Mater Electron (2017) 28:18873–18878
DOI 10.1007/s10854-017-7839-9

Preparation, structure and electrical properties of $La_{1-x}Ba_xCrO_3$ NTC ceramics

Mingxing Chen[1,2] · Huimin Zhang[1] · Ting Liu[1,2] · Hui Jiang[1] · Aimin Chang[1]

Received: 8 August 2017 / Accepted: 30 August 2017 / Published online: 4 September 2017

Abstract The $La_{1-x}Ba_xCrO_3$ (x = 0–0.2) negative temperature coefficient (NTC) ceramics have been prepared by the traditional solid-state reaction method at 1600 °C. Scanning electron microscope images show that the doping of Ba^{2+} contributes to the increase in the density. X-ray diffraction analysis has revealed that the sintered ceramics crystallize in a single perovskite structure. X-ray photoelectron spectroscopy analysis confirm the existence of Cr^{3+} and Cr^{6+} ions on lattice sites, which result in hopping conduction. The presence of the Cr^{3+} and Cr^{6+} ions is one of the significant factors that affect the electrical conductivity of $La_{1-x}Ba_xCrO_3$ ceramics. The resistance of NTC thermistors decreases with the increase of Ba content as a result of the enhancement of Cr^{6+} Concentration. The obtained values of ρ_{-50}, $B_{-50/-25}$ and E_a are in the range of 49.278–1.9839 × 10^5 Ω cm, 1767.4–3496.9 K, 0.1523–0.3013 eV, respectively.

1 Introduction

The $LaCrO_3$ is a refractory oxide with a high melting point (>2400 °C) and a distorted perovskite structure with orthorhombic symmetry (Pnma, space group 62) at room temperature [1]. It exhibits excellent chemical stability in both oxidizing and reducing atmospheres, and a good conductivity [2]. The lanthanum chromite-based ceramics gain interest for a variety of high-temperature electrochemical applications including interconnector in solid oxide fuel cell [3], thin film electric heaters [4], energy-saving material [5], composite thermistor ceramics [6] and so on. There are some mechanism of lanthanum chromite solid solutions that has been widely investigated for stabilizing phase transformation [7], optimizing sintering behavior [8], and modifying electrical properties [9]. Most frequently, the divalent alkaline earth cations dope $LaCrO_3$, such as Mg^{2+} [10, 11], Ca^{2+} [5, 12], Sr^{2+} [13, 14] and so on. What's more, $LaCrO_3$ doped with appropriate impurity ions can be applied as the NTC thermistor materials [15].

However, it is well known that it is very difficult to sinter $LaCrO_3$ ceramics in air atmosphere [16]. In order to enhance the density of $LaCrO_3$, the A-site and B-site were doped, such as $La_{1-x}Sr_xCrO_3$ [17], $LaCr_{1-x}Co_xO_3$ [1] and so on. This article will introduce that the A-site is doped by Ba^{2+} for adjusting the electrical properties and density of $LaCrO_3$.

2 Experimental procedures

The $La_{1-x}Ba_xCrO_3$ powders were synthesized by conventional solid-state method at 1200 °C for 5 h. High-pure lanthanum oxide (La_2O_3, purity >99.99%, Sinopharm Chemical Reagent co., Ltd, China), Chromium oxide (Cr_2O_3, purity >99%, Sinopharm Chemical Reagent co., Ltd, China), and Barium carbonate ($BaCO_3$, purity >98%, Sinopharm Chemical Reagent co., Ltd, China) were used as the initial raw material. According to the stoichiometry of $La_{1-x}Ba_xCrO_3$, the La_2O_3, Cr_2O_3 and $BaCO_3$ were well weighed, mixed, ground, and calcined at 1200 °C for 5 h. The calcined

✉ Huimin Zhang
zhanghm@ms.xjb.ac.cn

Aimin Chang
changam@ms.xjb.ac.cn

[1] Key Laboratory of Functional Materials and Devices for Special Environments of CAS, Xinjiang Key Laboratory of Electronic Information Materials and Devices, Xinjiang Technical Institute of Physics & Chemistry of CAS, Urumqi 830011, China

[2] University of Chinese Academy of Sciences, Beijing 100049, China

powders were then ground in mortar for 8 h. Subsequently, the powders were pressed into green pellets under a uniaxial pressure of 20 MPa to form the disks of 10 mm in a diameter, and then cold isostatic pressing at 200 MPa was used to enhance densities. The pressed disks were sintered in the temperature of 1600 °C for 5 h.

X-ray diffraction (XRD; BRUKERD8-ADVANCE, Cu K_α radiation) analysis was used to identify the crystalline phases of the sintered ceramic samples. Scanning Electron Microscope (SEM; Zeiss SUPRA 55 VP, Germany) was used to observe the microstructure of the sintered ceramic samples. X-ray photoelectron spectroscopy (XPS; Thermo, ESCALAB 250XI) was used to analyze the chemical states of the sintered ceramics. In order to obtain the electrical conductivity, the sintered ceramic samples were coated with some silver paste, and then annealed at 800 °C for 30 min. The resistance was measured in the temperature of −75 to 50 °C by Agilent 34970A multimeter in an oil bath. The density and open porosity of samples were measured by using Archimedes method.

3 Result and discussion

The XRD patterns and lattice constants of the sintered ceramics are shown in Fig. 1. Clearly, the samples of ceramics were consisted of a single phase isomorphic to the orthorhombic perovskite $LaCrO_3$ (JCPDS 24-1016). Typically no another phase occurred with the increase of Ba concentration in the ceramic samples. It indicates that the Ba^{2+} has all entered the perovskite lattice to form the solid solution in the process of high temperature sintering. From Fig. 1b, we can see that the lattice constants of sintered ceramics gradually increase with the increase of Ba^{2+} content. What's more, the diffraction peaks slightly shift toward lower angles with the increase of Ba^{2+} content. It indicates that the cell volume of the ceramic samples decrease with the increase of Ba^{2+} content according to the Bragg's Law:

$$2d\ \sin\theta = n\,\lambda \tag{1}$$

The main reason is that the ionic radius of substitution Ba^{2+} (0.135 nm) is greater than that of La^{3+} (0.1032 nm).

The SEM micrographs of the ceramics are shown in Fig. 2. As can be seen, there are many pores on the surface of sintered $LaCrO_3$ ceramics and the pores gradually decrease with the increase of Ba^{2+} content. Furthermore, the morphology of the grain gradually changes from a polyhedron into a cuboid. And the density of the sintered ceramics has been markedly improved with the increase of Ba^{2+}. The relative density of the sintered samples can be calculated by the following equation [1]:

$$\rho = \frac{\rho_{geom}}{\rho_{theor}} \tag{2}$$

The ρ_{geom} was obtained by Archimedes method. The ρ_{theor} was calculated as follows [1]:

$$\rho_{theor} = \frac{n \cdot \left[(1-x)M_{La} + xM_{Ba} + M_{Cr} + 3M_O\right]}{a \cdot b \cdot c \cdot N_A} \tag{3}$$

where n is the number of elements per unit cell ($n = 4$ for perovskite type $La_{1-x}Ba_xCrO_3$), N_A is the Avogadro constant, M_i is the atomic weight of element i (La, Cr, Ba, O). The a, b, c are the lattice constants which are calculated by XRD patterns. The ρ_{theor}, ρ_{geom}, relative density and open porosity for the $La_{1-x}Ba_xCrO_3$ ceramics are listed in Table 1. The relative density and open porosity of $La_{0.8}Ba_{0.2}CrO_3$ ceramics are 90.6 and 8%, respectively. Comparing with

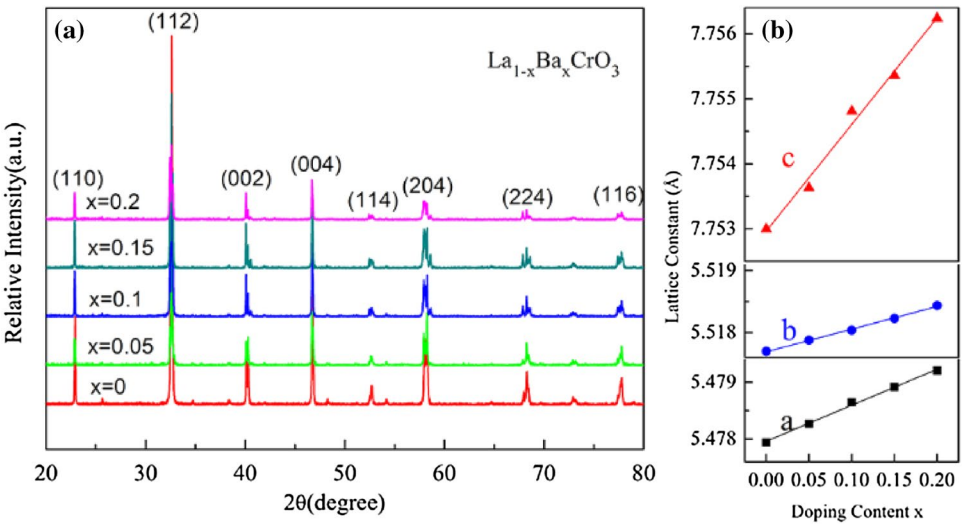

Fig. 1 **a** XRD patterns and **b** lattice constants of sintered $La_{1-x}Ba_xCrO_3$ (x = 0–0.2) ceramics

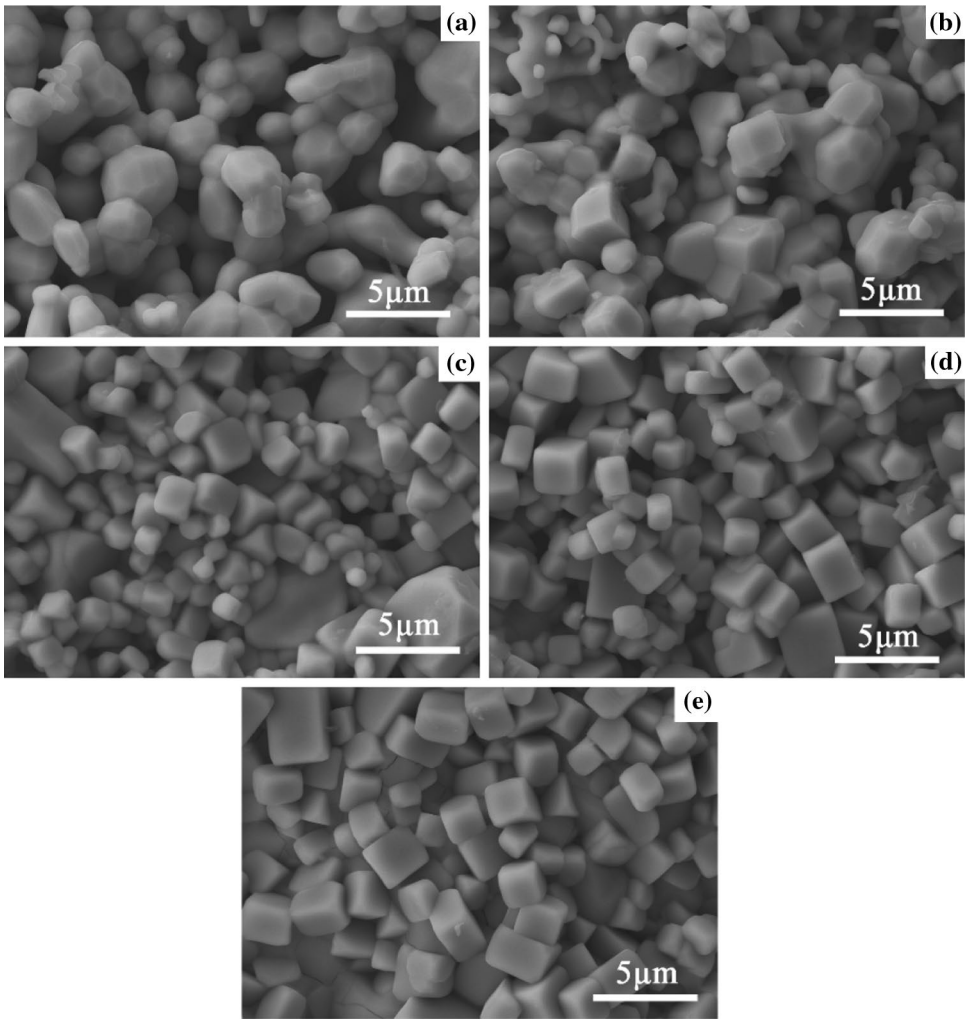

Fig. 2 SEM micrographs of the $La_{1-x}Ba_xCrO_3$ ceramics: **a** $x=0$, **b** $x=0.05$, **c** $x=0.1$, **d** $x=0.15$, **e** $x=0.2$

Table 1 The ρ_{theor}, ρ_{geom}, relative density and open porosity for the $La_{1-x}Ba_xCrO_3$ ceramics

x	ρ_{theor} (g/cm^3)	ρ_{geom} (g/cm^3)	Relative density (%)	Open porosity (%)
0	6.77367	4.07433	60.1	37
0.05	6.77026	4.85633	71.7	27
0.10	6.76633	5.58872	82.6	13
0.15	6.76301	6.00772	88.8	9
0.20	6.75945	6.12740	90.6	8

$La_{0.7}Ba_{0.3}CrO_3$ [9], the density of $La_{0.7}Ba_{0.3}CrO_3$ ceramic is 92% but there is the impure phase $BaCr_2O_4$. It may be that the doping content of Ba^{2+} exceeds the solid solution limit.

The XPS spectra of La 3*d* which is obtained from the sintered $La_{1-x}Ba_xCrO_3$ ceramic samples is shown in Fig. 3. It can be seen that the spectra peaks are associated with the presence of lanthanum in the form of La^{3+} [18]. Figure 4 shows the XPS spectra of Ba 3*d* obtained from the sintered ceramic samples. The spectra can be fitted using one component, which is characteristic of Ba^{2+} [19].

Figure 5 shows the XPS spectra and the curve-fitting example of ceramics in the regions of Cr 2*p* core-level peaks. As can be see, the peaks in the Cr $2p_{3/2}$ and Cr $2p_{1/2}$ spectra can be split into two peaks through Gaussian–Lorentzian curve fitting. The lower binding energy peak should be owing to Cr^{3+}, and the higher binding energy peak is the result of Cr^{6+}. The XPS results show that there are two different Cr ions in these samples, mainly Cr^{3+} and Cr^{6+}. The result is in good agreement with other authors [20]. What's more, the content of Cr^{6+} increases with the increase of Ba^{2+}. The reason is that the introduction of Ba^{2+} into the lattice could be compensated by the oxidation of Chromium ion from Cr^{3+} to Cr^{6+} just like the influence of doping Sr^{2+} [17].

Figure 6 shows the relationship of natural logarithm of the resistivity (ρ) and the reciprocal of absolute temperature (1000/*T*) for the NTC thermistors. It can be seen that the resistivity of sintered ceramics decreases with the increase of Ba^{2+}

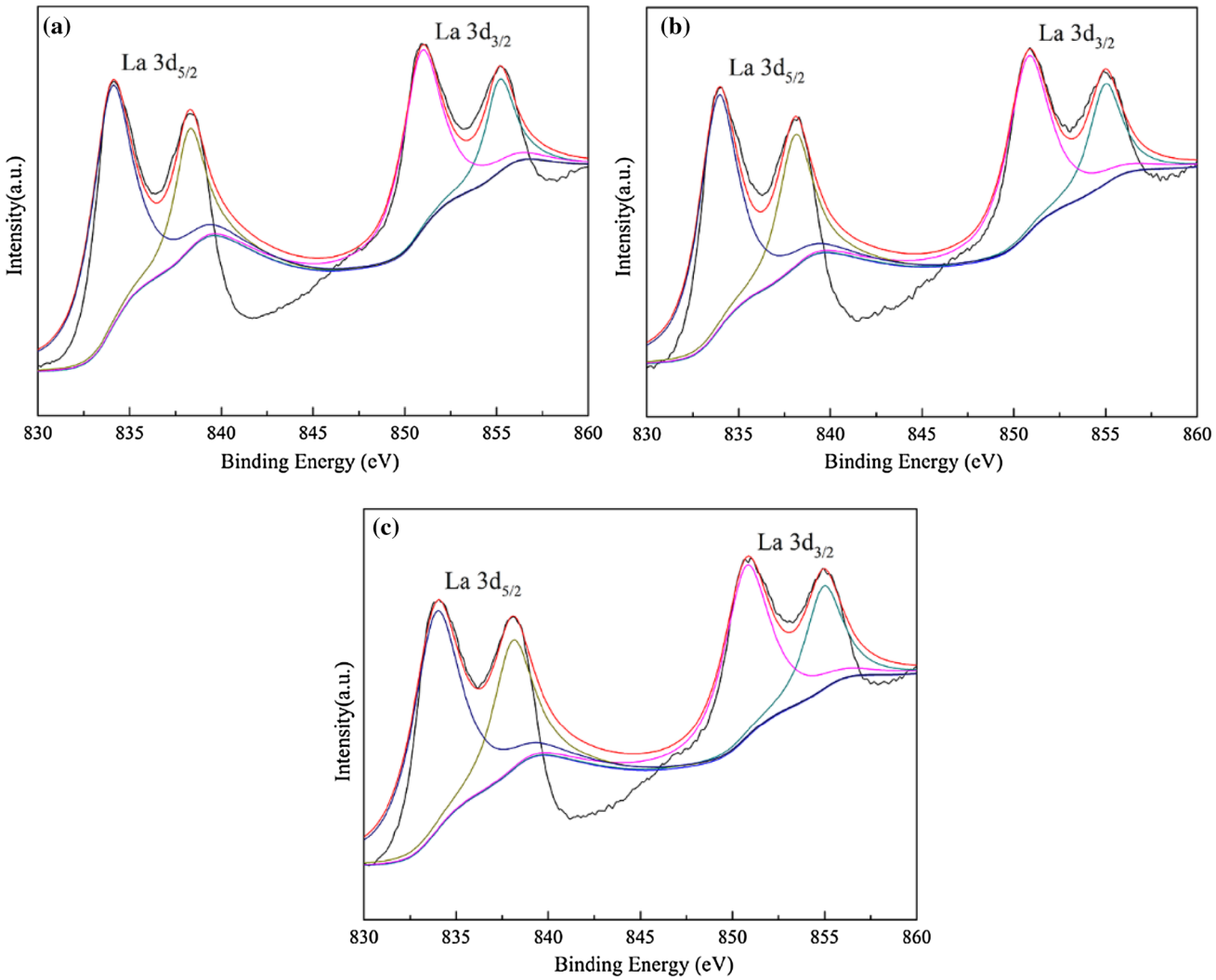

Fig. 3 La 3*d* XPS spectra collected for $La_{1-x}Ba_xCrO_3$ ceramics: **a** $x=0$, **b** $x=0.1$, **c** $x=0.2$

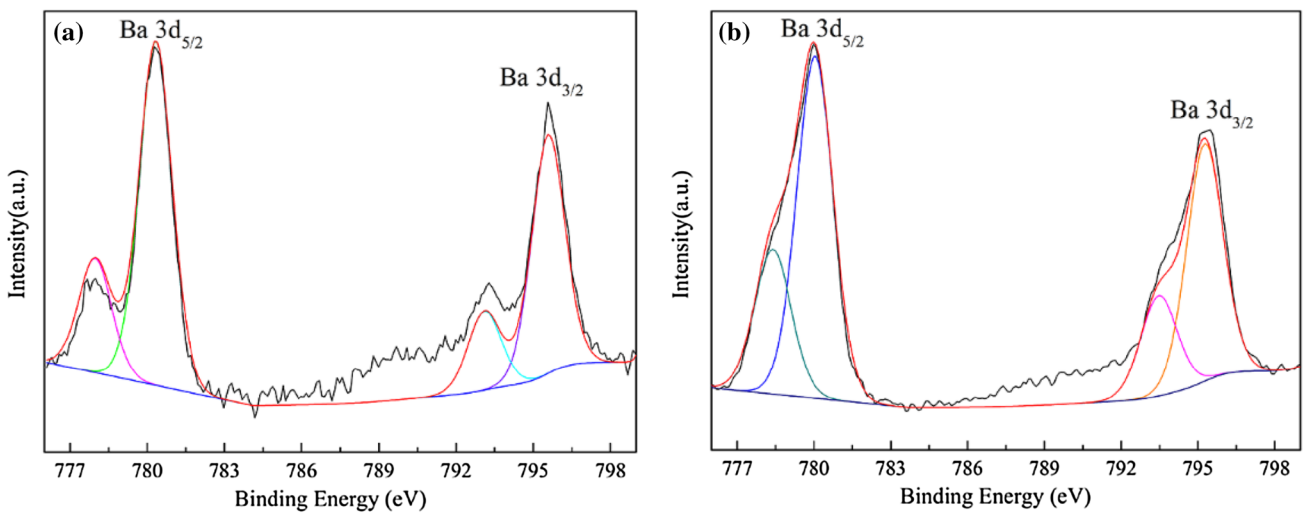

Fig. 4 Ba 3*d* XPS spectra collected for $La_{1-x}Ba_xCrO_3$ ceramics: **a** $x=0.1$, **b** $x=0.2$

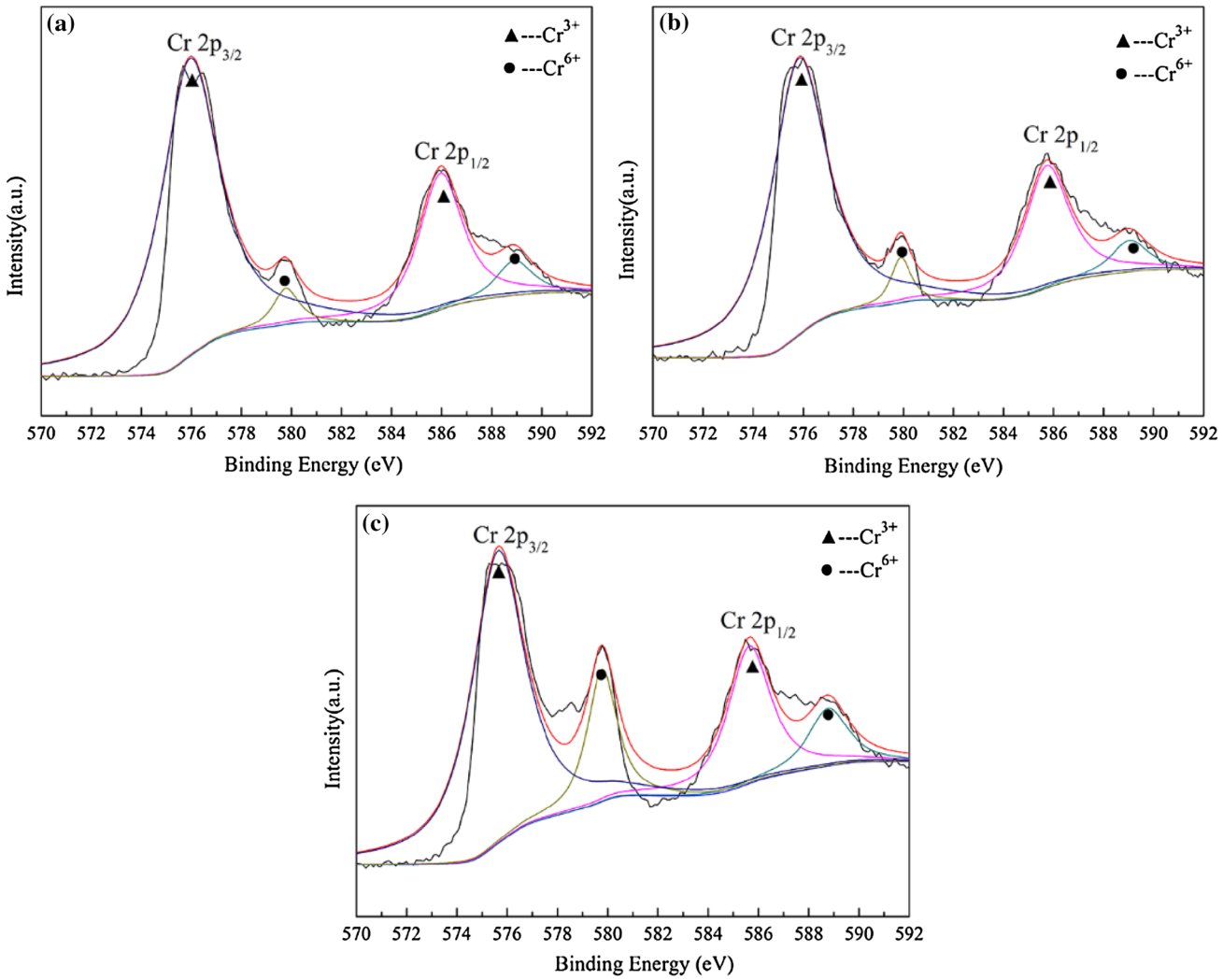

Fig. 5 XPS spectra results showing the Cr 2*p* regions of $La_{1-x}Ba_xCrO_3$ ceramics: **a** $x=0$, **b** $x=0.1$, **c** $x=0.2$. *Filled triangle* and *filled circle* indicate the peaks of the Cr 2*p* spectra attributed to Cr^{3+} and Cr^{6+}, respectively

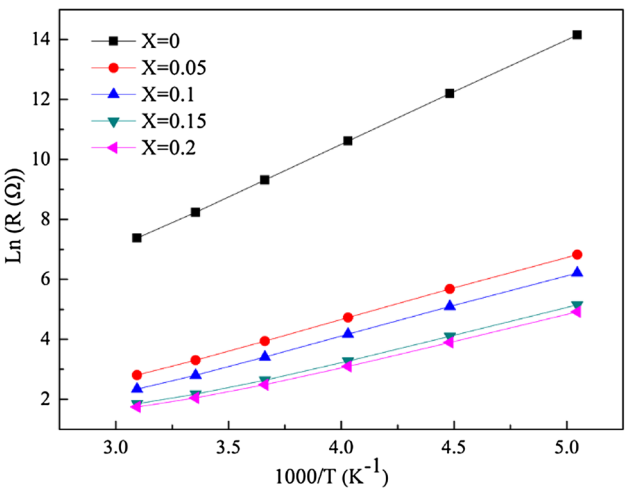

Fig. 6 The relationship between lnρ and 1000/T for the sintered $La_{1-x}Ba_xCrO_3$ ceramics

content. And the relationship of lnρ and 1000/T displays an approximate line in the measured temperature range. The linear dependence depends on the small-polaron hopping transport mechanism [21], which can be described by the Arrhenius relationship [22]:

$$\rho = \rho_0 \exp\left(\frac{E_a}{kT}\right) \tag{4}$$

where ρ_0 is the resistivity at infinite temperature, E_a is the activation energy for electrical conduction, k is the Boltzmann constant, T is the absolute temperature. The thermal constant B which describes the temperature sensitivity of material can be calculated as follows [22]:

$$B = \left[\frac{T_1 T_2}{T_2 - T_1}\right] \ln\left(\frac{R_1}{R_2}\right) \tag{5}$$

Table 2 Resistivity at a temperature of 50 °C (ρ_{-50}), thermal constant ($B_{-25/-50}$) and activation energy for the $La_{1-x}Ba_xCrO_3$ NTC thermistor

x	ρ_{-50} (Ω cm)	$B_{-25/-50}$ (K)	Ea (eV)
0	198394.6	3496.9	0.3013
0.05	293.1	2104.5	0.1814
0.10	163.6	2048.7	0.1765
0.15	60.5	1826.8	0.1574
0.20	49.3	1767.4	0.1523

where R_1 is the resistance at temperature T_1, and R_2 is the resistance at temperature T_2. The value of ρ_{-50}, $B_{-50/-25}$ and E_a are shown in Table 2. The value of ρ_{-50}, $B_{-50/-25}$ and E_a are in the range of $49.278–1.9839\times10^5$ Ω cm, 1767.4–3496.9 K, 0.1523–0.3013 eV, respectively. The electrical properties can be adjusted by adjusting the Ba^{2+} concentration.

4 Conclusions

The preparation, structure and electrical properties of $La_{1-x}Ba_xCrO_3$ ceramics have been investigated. The sintered ceramic samples are a single orthorhombic perovskite phase. The density of the sintered ceramics has been greatly improved by the doping of Ba^{2+}. The electrical conductivity of these sintered ceramics is that the polarons jumps between different oxidation states of chromium ions. The resistivity decreases with the increase of Ba^{2+} content. The values of ρ_{-50}, $B_{-25/-50}$ constant and activation energy Ea of the thermistors are in the range of $49.278–1.9839\times10^5$ Ω cm, 1767.4–3496.9 K, 0.1523–0.3013 eV, respectively. The electrical properties can be adjusted by adjusting the Ba^{2+} concentration. These materials could be used as potential candidates for NTC thermistors.

Acknowledgements This study was supported by the Autonomous Region Youth Science and Technology Innovation Personnel Training Project (No. QN2015JQ010).

References

1. A. Bonet, M. Baben, N. Travitzky, P. Greil, J. Am. Ceram. Soc. **99**, 917 (2016)
2. H. Yokokawa, N. Sakai, T. Kawada, M. Dokiya, J. Electrochem. Soc. **138**, 1018 (1991)
3. J. Sfeir, J. Power Sources **118**, 276 (2003)
4. Y. Ito, K. Wakisaka, H. Kado, S. Yoshikado, Key Eng. Mater. **301**, 171 (2006)
5. Z. Han, J. Liu, X. Li, Y. Chen, G. Liu, J. Li, J. Am. Ceram. Soc. **97**, 2705 (2014)
6. B. Zhang, Q. Zhao, A. Chang, Y. Wu, H. Li, J. Alloys Compd. **675**, 381 (2016)
7. M. Mori, Y. Hiei, N.M. Sammes, Solid State Ionics **135**, 743 (2000)
8. M. Iwasaki, H. Takizawa, K. Uheda, T. Endo, M. Shimada, J. Mater. Chem. **8**, 2765 (1998)
9. S.P. Jiang, L. Liu, K.P. Ong, P. Wu, J. Li, J. Pu, J. Power Sources **176**, 82 (2008)
10. B.K. Flandermeyer, M.M. Nasrallah, A.K. Agarwal, H.U. Anderson, J. Am. Ceram. Soc. **67**, 195 (1983)
11. K. Azegami, M. Yoshinaka, K. Hirota, O. Yamaguchi, Solid State Commun. **112**, 281 (1999)
12. Y. Fu, H. Wang, C. Weng, S. Hu, Y. Liu, J. Am. Ceram. Soc. **98**, 2561 (2015)
13. T. Takeuchi, Y. Takeda, R. Funahashi, T. Aihara, M. Tabuchi, H. Kageyama, J. Electrochem. Soc. **147**, 3979 (2000)
14. H. Qi, Y. Luan, S. Che, L. Zuo, X. Zhao, C. Hou, Inorg. Chem. Commun. **66**, 33 (2016)
15. K. Azegami, M. Yoshinaka, K. Hirota, O. Yamaguchi, J. Electrochem. Soc. **147**, 2830 (2000)
16. L. Groupy, H.U. Anderson, J. Am. Ceram. Soc. **59**, 449 (1976)
17. X. Liu, W. Su, Z. Lu, J. Liu, L. Pei, W. Liu, L. He, J. Alloys Compd. **305**, 21 (2000)
18. H. Berthou, C.K. Jørgensen, C. Bonnelle, Chem. Phys. Lett. **38**, 199 (1976)
19. H. Van Doveren, J.A.T.H. Verhoeven, J. Electron. Spectrosc. Relat. Phenom. **21**, 265 (1980)
20. L. Li, Q. Wei, Z. Kang, M. Rui, W. Su, J. Alloys Compd. **249**, 264 (1997)
21. A.N. Kamlo, J. Bernard, C. Lelievre, D. Houivet, J. Eur. Ceram. Soc. **31**, 1457 (2011)
22. A. Feteira, J. Am. Ceram. Soc. **92**, 967 (2009)